

Effects of Impulse Voltage Polarity, Peak Amplitude and Rise-Time on Streamers Initiated from a Needle Electrode in Transformer Oil

J. Jadidian, *Student Member, IEEE*, M. Zahn, *Fellow, IEEE*, N. Lavesson, O. Widlund and K. Borg

Abstract—An electro-thermal hydrodynamic model is presented to evaluate effects of the applied lightning impulse voltage parameters such as polarity, magnitude, and rise-time on the initiation and propagation of the streamers formed in an IEC defined needle-sphere electrode geometry filled with transformer oil. Instantaneous velocity, column diameter, head curvature, maximum electric field, and the volume charge density have been investigated as the main characteristics of the streamer. Modeling results indicate that greater applied voltage peak amplitudes form streamers with higher velocity, greater head curvatures and thicker columns. The bushy negative streamers usually initiate at almost twice the applied voltage magnitude and propagate slower than filamentary positive streamers. Results also show that in transformer oil at the same impulse voltage peak amplitude, shorter rise-times create thicker positive and negative streamers.

Index Terms—Dielectric breakdown, transformer oil, streamers, impulse lightning voltage.

I. INTRODUCTION

Transformer oil is of high technical interest in compact pulsed power technologies, high voltage insulation and power apparatus cooling due to its electrical breakdown strength and thermal cooling capabilities which are considerably greater than gaseous insulators, while its ability to conform to complex geometries means that they are often of more practical use than solid insulators. The phenomenology of liquid breakdown has been the subject of theoretical and experimental studies for many years but still is not fully understood [1]-[6]. Electrical breakdown in liquid dielectrics is carried out by streamers with low-density conductive structures, which form in regions of the liquid that are electrically over-stressed (1×10^8 V/m or greater) [1]-[6]. Formation of streamers in transformer oil is due to the field dependent molecular ionization of hydrocarbon molecules at intense electric field [5]-[7]. The extent of a streamer also depends upon the characteristics of the pulsed electrical excitation such as polarity, magnitude, duration, rise time, etc. This paper investigates the breakdown physics of transformer oil using an electro-thermal hydrodynamic model. Positive and negative streamers are compared in a needle-sphere electrode geometry defined by IEC 60897 as shown in Fig. 1.

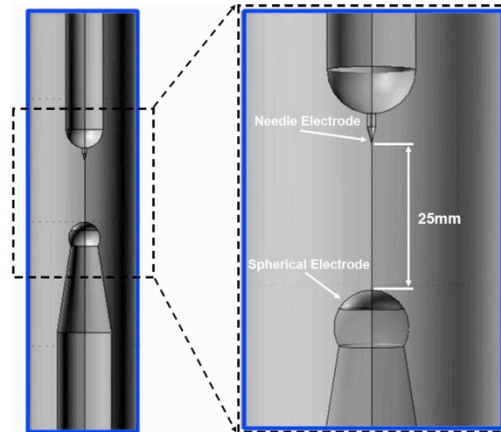


Figure 1: Needle-sphere electrode geometry used for streamer simulation purposes as described in IEC 60897 standard [8]. The electrodes are 25 mm apart and radii of curvature of the needle electrode and the spherical electrode are 40 μm and 6.35 mm, respectively.

The basic structure of the two-dimensional (2D) axis-symmetric model developed in this paper is analogous to those used in [5], [6]; however, several key improvements have been made in the present version of the model, including:

- Lightning impulse voltages (based on IEC standard definition [9]) have been applied instead of Heaviside step functions used in [5], [6] to make the results comparable to the experimental records.
- Effects of the electric field on the hydrocarbon molecules ionization potential are taken into account based on results derived from quantum chemistry theories [7].
- More consistent stabilization techniques have been employed to solve the conservation of charge equations for each charge carrier.
- Different combinations of direct and iterative solvers have been employed which enables the model to solve the equations with much greater spatial resolutions.

This paper is organized with Section II describing the governing equations and the boundary equations of the electro-thermal hydrodynamic model as well as a detailed description of the electric field dependent molecular ionization. Section III gives the results of the streamer model for different polarities and peak amplitudes. The effects of the applied voltage rise-times on the positive and negative streamers are discussed in Section IV. Section V addresses the weak points of the model mostly pertaining to the molecular properties of the dielectric liquid. The paper concludes in Section VI with a summary of the key results of the model.

II. GOVERNING EQUATIONS AND BOUNDARY CONDITIONS

A three-carrier continuum model is utilized to account for the charge generation and capture mechanisms, which are critical in the study of streamers. The governing equations that contain the physics to model streamer development are based on the drift-dominated charge continuity equations (1)-(3) for positive ion (ρ_p), negative ion (ρ_n) and electron (ρ_e) charge densities, coupled through Gauss' law (4). The thermal diffusion equation (5) is included to model temperature variations (T) and gas formation in oil. The negative ion and electron charge densities are both negative quantities.

$$\frac{\partial \rho_p}{\partial t} + \nabla \cdot (\rho_p \mu_p \bar{E}) = G_M(|\bar{E}|) + \frac{\rho_p \rho_e R_{pe}}{q} + \frac{\rho_p \rho_n R_{pn}}{q} \quad (1)$$

$$\frac{\partial \rho_n}{\partial t} - \nabla \cdot (\rho_n \mu_n \bar{E}) = \frac{\rho_e}{\tau_a} - \frac{\rho_p \rho_n R_{pn}}{q} \quad (2)$$

$$\frac{\partial \rho_e}{\partial t} - \nabla \cdot (\rho_e \mu_e \bar{E}) = -G_M(|\bar{E}|) - \frac{\rho_p \rho_e R_{pe}}{q} - \frac{\rho_e}{\tau_a} \quad (3)$$

$$\nabla \cdot (\varepsilon \bar{E}) = \rho_e + \rho_p + \rho_n, \quad \bar{J} = (\mu_p \rho_p - \mu_e \rho_e - \mu_n \rho_n) \bar{E} \quad (4)$$

$$\frac{\partial T}{\partial t} + v \cdot \nabla T = \frac{1}{\rho_l c_v} (k_T \nabla^2 T + \bar{E} \cdot \bar{J}) \quad (5)$$

where v , ε , k_T , c_v , and ρ_l are the oil's velocity, permittivity ($2.2 \varepsilon_0$), thermal conductivity, specific heat, and mass density, respectively. Representative values for transformer oil can be found in Table I. In the microsecond time scales of interest for streamer formation, the oil's velocity is negligible such that $v = 0$. Also, q is the magnitude of electronic charge and E is the local electric field. The parameters μ_p , μ_n , and μ_e are the mobilities of the positive ions, negative ions and electrons respectively. The values of mobilities are taken from primary references of [6]. R_{pn} and R_{pe} are the ion-ion and ion-electron recombination coefficients obtained from the Langevin relationship $R_{pn} = R_{pe} = q(\mu_p + \mu_n)/\varepsilon$ [5]. The two rates are assumed equal since using the Langevin relationship for the ion-electron recombination rate leads to overestimation. The Langevin recombination relationship is a diffusion limited process and valid for situations where the electric field levels are low to moderate and the recombining species are of similar physical scale. To compensate for the reduction in the recombination cross-section caused by high electric field levels, we have used the Langevin recombination term for ion-ion recombination to model ion/electron recombination.

This approach effectively compensates for the reduction in the recombination cross-section by reducing the apparent electron mobility. In addition to recombination, electrons also combine with neutral molecules to form negative ions. This process is described as an electron attachment time constant, $\tau_a = 200$ ns [8].

The generation and recombination terms play a key role in describing streamer dynamics. In spite of the recombination terms that are defined by constants, the field ionization charge density rate source term, G_M , is modeled using the Zener model of electron tunneling in solids [11]:

$$G_M(|\bar{E}|) = \frac{q^2 n_0 a |\bar{E}|}{h} \exp\left(-\frac{\pi^2 m^* a IP(\bar{E})^2}{qh^2 |\bar{E}|}\right) \quad (6)$$

Parameter $h = 6.626068 \times 10^{-34}$ m²kg s⁻¹ is the Planck's constant. The other parameter values as listed in Table I are consistent with those used in [5], [6] except electric field dependent ionization potential, $IP(\bar{E}) = \Delta - \gamma \sqrt{|\bar{E}|}$, which has been derived by Density Functional Theory (DFT) [12]. Smalø *et al.* have used DFT to find out the effect of the intense electric field on the ionization energy of hydrocarbons [7]. The ionization energy for the different aromatic, naphthenic and paraffinic hydrocarbon molecules, are derived and fitted by linear regression. Models that use generation term in Eq. (6) with constant ionization potential, IP [5], [6] are not able to describe positive streamers formed by extremely high voltages (above +200 kV) and negative streamers. By importing the electric field dependent ionization potential function derived by DFT into Eq. (6), we have:

$$G_M(|\bar{E}|) = \frac{q^2 n_0 a |\bar{E}|}{h} \exp\left(-\frac{\pi^2 m^* a \left(\frac{\Delta}{\sqrt{|\bar{E}|}} - \gamma\right)^2}{qh^2}\right) \quad (7)$$

Application of the generation term in the form of Eq. (7) in Eq. (1), and Eq. (3) enables the model to describe the negative streamers and positive streamers formed by extra high voltages (≥ 200 kV) [15]. Representative parameter values for the ionization potential function are listed in Table I as well as other parameters used to solve governing equations (1-6).

TABLE I
PHYSICAL PARAMETERS USED IN THE STREAMER MODEL

Symbol	Parameter	Value
n_0	Number density of ionizable species	1×10^{23} m ⁻³ [4,5]
a	Molecular separation distance	3.0×10^{-10} m [4,5]
m^*	Effective electron mass	$0.1 \times m_e = 9.1 \times 10^{-32}$ kg [24]
Δ, γ	Ionization potential function parameters	1.16×10^{-18} J, 1.118×10^{-23} Jm ^{1/2} V ^{-1/2} [7], [12]
R_{pn}, R_{pe}	Ion-ion and ion-electron recombination rates	1.64×10^{-17} m ³ s ⁻¹ [5]
μ_p, μ_n	Positive and negative ion mobilities	10^{-9} m ² V ⁻¹ s ⁻¹ [6]
μ_e	Electron mobility	10^{-4} m ² V ⁻¹ s ⁻¹
c_v	Specific heat	1.7×10^3 Jkg ⁻¹ K ⁻¹
ρ_l	Oil mass density	880 kgm ⁻³
k_T	Thermal Conductivity	0.13 Wm ⁻¹ K ⁻¹
q	Electronic charge	1.602×10^{-19} C

Consistent boundary conditions have been applied to the streamer model. The potential of the sphere electrode is set to the ground. The needle electrode potential is defined using two subtracting exponential voltages to create the standard lightning impulse voltage according to IEC 60060-1 [9] as:

$$V_{impulse} = KV_0 \left(e^{-\frac{t}{\tau_1}} - e^{-\frac{t}{\tau_2}} \right) \quad (8)$$

where K is a non-dimensional compensation factor to determine the polarity of impulse voltage and to keep the peak amplitude of the impulse approximately equal to V_0 , since in general, the maximum value of subtraction of two exponential functions is not generally 1.

The top, bottom and side insulating walls shown in Fig. 1 have been assigned to have zero normal displacement field components ($\vec{n} \cdot \vec{D} = 0$). This boundary condition acts like a continuity equation, which means no terminating walls are felt by electric field lines across the walls. The electrode boundary conditions along the charge transport continuity equations are convective fluxes for all species, while insulating wall boundaries are assigned to have no flux of any species. All boundaries are set to zero normal thermal diffusive flux (i.e., $\vec{n} \cdot \vec{\nabla} T = 0$) making the approximation that the system is adiabatic on the timescales of interest.

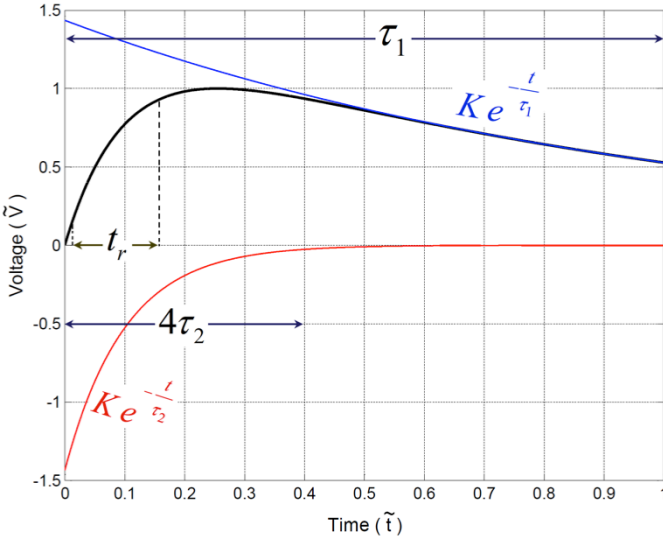


Figure 2: IEC 60060 lightning impulse voltage (non-dimensional, $\tilde{V} = V/V_0$) with rise-time t_r (10% to 90% of peak voltage) versus non-dimensional time, $\tilde{t} = t/\tau_1$, generated with subtracting two exponential functions.

Since diffusion of the charged species is assumed to be negligible in Eq. (1-3), we have solved the conservative form of the general convection and diffusion equations with triangular quartic elements. Numerical solutions of the charge continuity equations usually exhibit harsh oscillations given that the exact solutions are smooth and continuous. These spurious oscillations are caused by numerical instabilities [13], [14]. To avoid these severe local oscillations that exist in the

number density of charged species of previous model [5], [6], which has been solved using only the artificial anisotropic streamline diffusion (AISD) formulation for the scalar convection-diffusion equation, nonlinear crosswind diffusion (CWD) has been applied as an artificial diffusion stabilizer in addition to different types of streamline diffusions (SDs) such as (anisotropic, compensated streamline upwind Petrov-Galerkin (SUPG) and Galerkin least-square methods) to solve the charge continuity equations. It has been shown in [13] that CWD is less over-diffusive than other discontinuity-capturing techniques and leads to a better numerical behavior, while it is computationally expensive due to its non-linear nature [14]. On the other hand, SD techniques effectively stabilize the system and accelerate the solution. We have applied both SD and CWD at the same time to optimally stabilize the numerical solution [14]-[16]. Both artificial diffusion techniques are tuned to balance a tradeoff between removing nonphysical local oscillations (due to SD) and excessively smooth results just next to the walls (due to CWD). An average has been taken whenever any discrepancy is observed between results of different SD techniques mentioned above.

Two direct solvers, MUMPS and PARADISO are employed separately to solve the streamer model. These solvers are well known to be robust and memory efficient tools in parallel high performance computing [14]. Solutions of these solvers are in an excellent agreement for 10^6 degrees of freedom. These direct solvers have the advantage of more accuracy compared to iterative solvers, and on the other hand, they are computationally much more expensive. Since the present model contains nonsymmetrical matrices and nonlinear equations (due to the CWD), combinations of direct and iterative solves have been applied to speed up the solution of the model. Three computer machines with a total 36 threads (~ 3.4 GHz) and 188 GB are used in parallel to solve Eq. (1)-(7) with given boundary conditions.

III. EFFECTS OF POLARITY AND PEAK AMPLITUDE

It has been experimentally observed that streamer propagation characteristics are strongly dependent on the voltage polarity and peak amplitude [1]-[3]. In the case of transformer oil, experimental evidence has shown that streamers emanating from a positive electrode tend to initiate at lower applied voltages and propagate faster and further than negative streamers [1]-[3]. A few streamer propagation modes have been identified for lightning impulse voltage excitations depending on the peak amplitude of the excitation voltage. For instance, the 2nd mode positive streamers initiate at the breakdown voltage, which denotes 50% probability of breakdown, while the 3rd mode initiates at the acceleration voltage (roughly 2 times greater than 50% breakdown voltage) where the streamer propagation velocity rises dramatically [2], [3]. Average propagation velocities for 2nd and 3rd mode streamers are on the order of 1 km/s and 10 km/s respectively [2], [3]. In the literature, the 1st mode of positive streamers is often ignored as it has a low probability of leading to breakdown [6]. Similar modes have been defined for negative

streamers depending on applied voltage magnitude [2]. Simulation results clearly show the effects of applied voltage peak for both polarities. Figure 3 shows a filamentary positive streamer formed by an applied voltage with +130 kV peak and 100 ns rise-time at $t=155$ ns. The initiation velocity and diameter of this streamer are clearly less than a positive streamer formed by an applied voltage with +200 kV peak and 100 ns rise-time shown at $t=100$ ns in Fig. 4. The effect of the applied voltage peak is even more evident in Fig. 5 showing a higher mode positive streamer formed by an applied voltage with +400 kV peak and 100 ns rise-time shown at $t=100$ ns. The average velocity of +400 kV is at is approximately greater by factors of 4 and 2 than +200 kV and +130 kV respectively. In addition, it can be seen in these figures that higher applied voltages create thicker positive streamers.

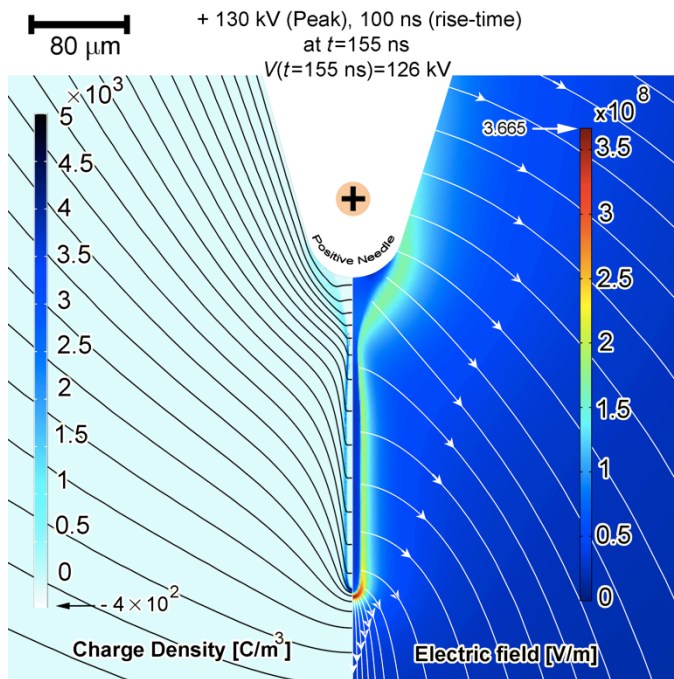


Figure 3: Electric field magnitude and lines (right side) and the net charge density and equipotential lines (left side) for a positively applied lightning impulse voltage with 130 kV peak and 200 ns rise-time at $t=155$ ns. No discharges are observed for a 130 kV negatively applied impulse voltage.

Positive streamers formed by +130 kV and +200 kV impulse voltages (shown in Figs. 3 and 4) almost reached their eventual diameters after the streamer head travels about 250 μm from the positive needle tip. However, it takes relatively longer time for +400 kV streamer to attain its ultimate diameter. This streamer is shown after 200 ns in Fig. 6, when the variation of the streamer diameter is almost damped. We will further discuss the positive streamer diameters in Section IV.

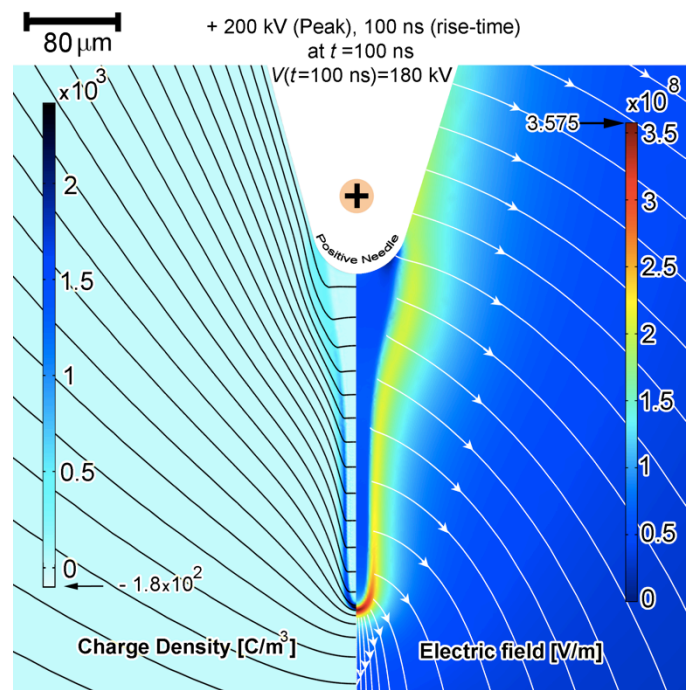


Figure 4: Electric field magnitude and lines (right side) and the net charge density and equipotential lines (left side) for a positively applied lightning impulse voltage with 200 kV peak and 100 ns rise-time at $t=100$ ns.

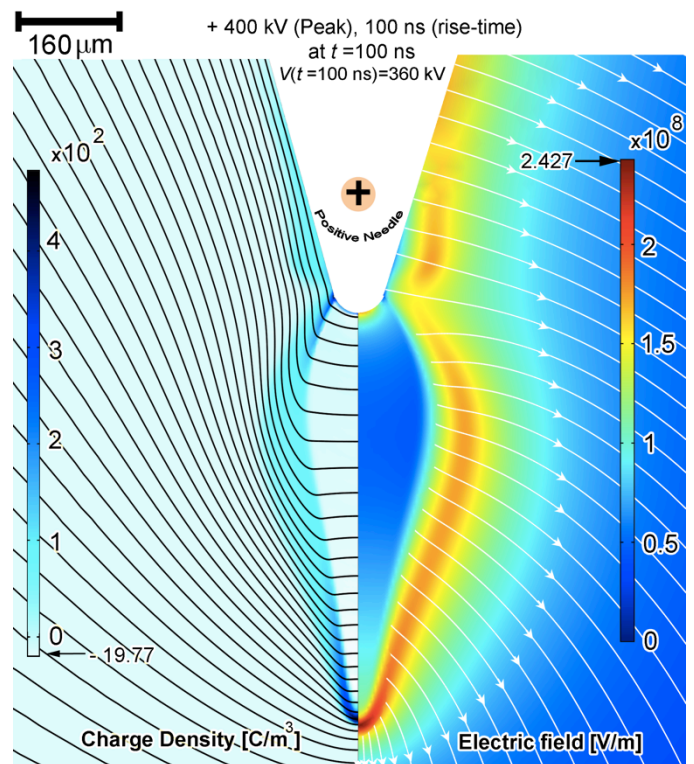


Figure 5: Electric field magnitude and lines (right side) and the net charge density and equipotential lines (left side) for a positively applied lightning impulse voltage with 400 kV peak and 100 ns rise-time at $t=100$ ns.

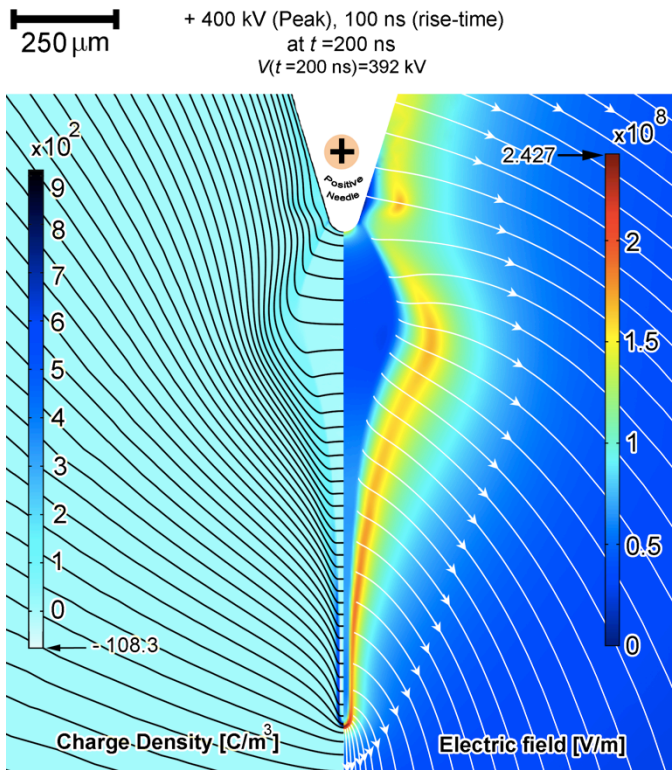


Figure 6: Electric field magnitude and lines (right side) and the net charge density and equipotential lines (left side) for a positively applied lightning impulse voltage with 400 kV peak and 100 ns rise-time at $t=200$ ns.

In spite of filamentary positive streamers, negative streamers form in a bushy shape as shown in Figs. 7 and 8. The negative streamer produced by an impulse with -400 kV peak and 1 ns rise-time grows in both axial and radial directions to build an ionized bubble in the vicinity of the negative needle. Such a bushy configuration of the net charge density significantly shields the intense electric field, which leads to a significant drop in the streamer velocity after the streamer front travels about half a millimeter from the needle tip. The negative streamers cannot initiate in a filamentary shape, since the opposing electric field formed by stationary ions slows down the electrons; while in positive streamers, sluggish positive ions assist the electric field amplification ahead of the streamer, which accelerates the filamentary streamer even at a few millimeter from the needle tip.

Increasing the applied voltage peak amplitude affects negative streamer shape and the velocity of negative streamers fairly similar to the positive counterparts. Figure 8 shows a negative streamer formed by an applied voltage with -600 kV and 1 ns rise-time. Comparing Figs. 7 and 8 clarifies that higher voltages create a bulkier ionized bubble, which grows faster, and further in both axial and radial directions. As can be seen in Fig. 7 and 8, the negative streamers occupy much more volume since the highly mobile electrons are repelled by the negative needle electrode and migrate into the liquid bulk. On the other hand, applied positive impulse voltage extracts the electrons from the ionization zone back to the needle electrode creating a positive space charge region that reduces

the electric field near the needle electrode and enhances the electric field ahead of the positive space charge region. The field enhancement makes the positive streamer initiation possible at lower applied voltage peak amplitudes compared to the negative streamers.

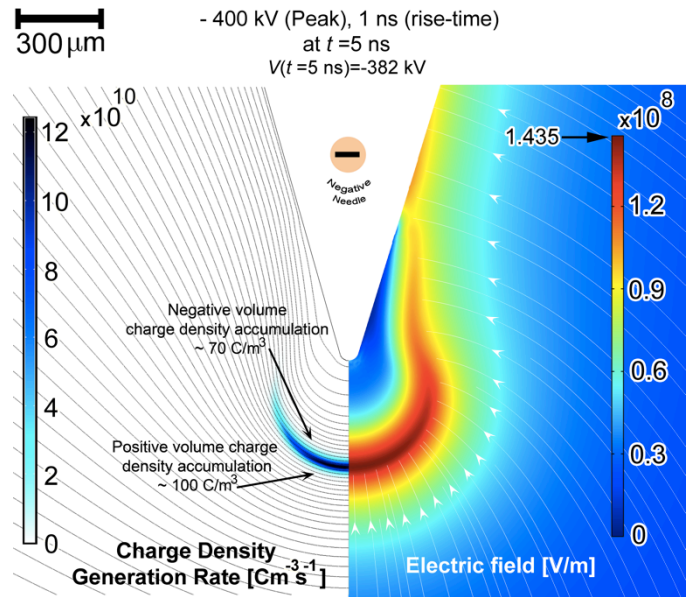


Figure 7: Electric field magnitude and lines (right side) and the net charge density and equipotential lines (left side) for a negatively applied lightning impulse voltage with -400 kV peak and 1 ns rise-time at $t=5$ ns.

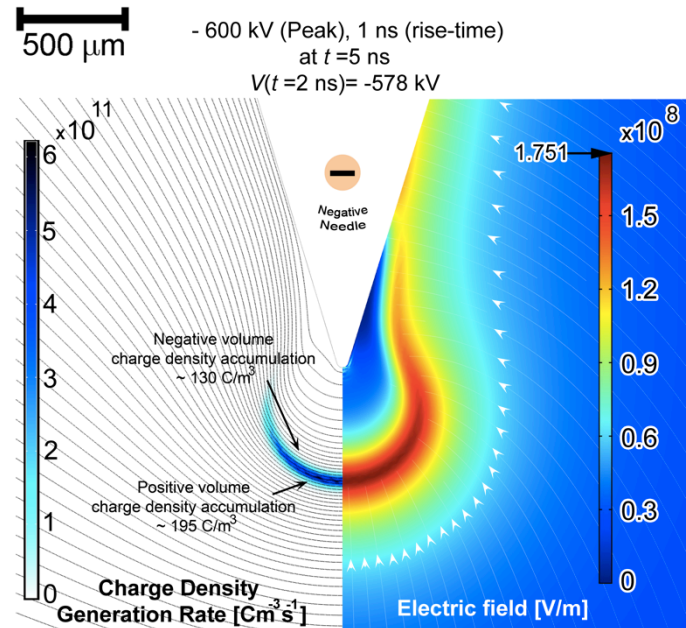


Figure 8: Electric field magnitude and lines (right side) and the net charge density and equipotential lines (left side) for a negatively applied lightning impulse voltage with -600 kV peak and 1 ns rise-time at $t=2$ ns.

The model reveals that the velocity and the shape of positive streamers are approximately insensitive to the changes in electron mobility as long as it is about two orders of magnitude greater than the ion mobilities. The experimental results confirm this prediction of the model as reported in [17]. However, the shape and the velocity of negative streamers are

quite sensitive to the electron mobility.

The main difference in the effects of the higher applied voltage peak amplitudes between positive and negative streamers is that the higher positive applied voltage peaks lead to an increase in streamer velocity and streamer diameter and not the electric field ahead of the ionized region while in negative streamers both electric field ahead of the ionized body and the streamer velocity are increased by higher negative peaks as can be seen in Figs. 4-8.

Ionizing the oil molecules into slow positive and negative ions and fast electrons quickly develops a net volume charge because the highly mobile electrons are swept away from the ionization zone leaving behind the low mobility positive and negative ions. The net charge density at the streamer crust, with the same polarity as the needle electrode, modifies the electric field distribution in the oil such that the electric field close to the needle electrode decreases while the electric field magnitude ahead of the ionized volume in the oil increases. The new enhanced electric field distribution leads to ionization occurring further away from the needle electrode, which in turn causes further modification of the electric field and charge distributions. The ultimate result of these electrodynamic processes is the development of an ionizing electric field front, which is a moving dissipative charge carrier source due to the collisions, raises the temperature to vaporize transformer oil and create a gas phase. The temperature rise in the negative streamers is considerably greater over a larger volume. Experimental results have shown that negative streamers initiated from the needle electrode generate gas bubbles around the needle with diameters on the order of 1-mm in transformer oil [18]-[20]. These observations support the numerical results of our model obtained for negative streamers, since in the larger ionized body around the negative needle, the temperature is about 5000 K, about one order of magnitude higher than the boiling point of the transformer oil (~500 K). Therefore, it is reasonable to think of a vapor phase generated inside the bushy ionized body around the negative needle. On the other hand, since the volume that must be ionized by negatively applied impulse voltage is much larger, the negative streamers demand more energy to form. As a consequence, negative streamer formation occurs at a higher impulse voltage peak than their positive counterparts.

Figure 9 shows the distance of the streamer head from the needle tip for positive and negative streamers initiated by different applied voltage peaks. Error-bars in Fig. 9 show the range of results obtained by application of different streamline artificial diffusions (anisotropic, compensated streamline upwind Petrov-Galerkin (SUPG) and Galerkin least-square methods) to solve continuity equations and the curves are plotted by taking averages on the results of these artificial stabilization techniques. The streamer velocity under +400 kV is roughly 2 times greater than +200 kV streamer velocity which itself is 2 times greater than +130 kV streamer velocity.

The velocity of the negative streamers is initially higher than positive streamers, however, the instantaneous velocity of a positive streamer tends to increase after a few tens of

nanoseconds, before the streamer reaches ~1.2 mm from the needle, while the negative streamer velocity decreases significantly after the initial bubble formed around the needle.

At the point 1.5 mm from the needle, the streamer velocities are ~2.5 km/s, 5 km/s, 12 km/s, 1 km/s and 3 km/s for streamers formed by applied voltage peaks of +130 kV, +200 kV, +400 kV, -400 kV and -600 kV respectively which correspond well with experimental results of [2], [3] and [17].

Beyond ~1.5 mm from the needle both positive and negative streamer velocities gradually decrease. The positive streamer velocity falls to ~1 km/s, ~3.5 km/s and ~6 km/s for 130 kV, 200 kV and 400 kV applied voltage peaks respectively, which are again in good agreement with corresponding experimental results of [2]-[4] and [17].

It has also been presented in [2] that initiation velocities of 3rd mode positive streamers (occurring above 200 kV in a 25 mm gap) are at most 2~3 times greater than 2nd mode. The dramatic rise in positive streamer propagation velocity only appears when the 3rd mode streamer head travels about 8~10 mm from the needle tip [3] which is not covered in Fig. 9. Our 2-D axisymmetric model is unable to keep track of the streamer head velocity this far, since at these points branching usually happens [2]. The branching phenomenon is one of the most interesting characteristics of the streamers in dielectrics, which is not physically understood. The present 2-D axisymmetric model is not able to keep the track of the off-axis branches emanating from the main streamer root, since it forces the entire streamer development process to stay in axial symmetry.

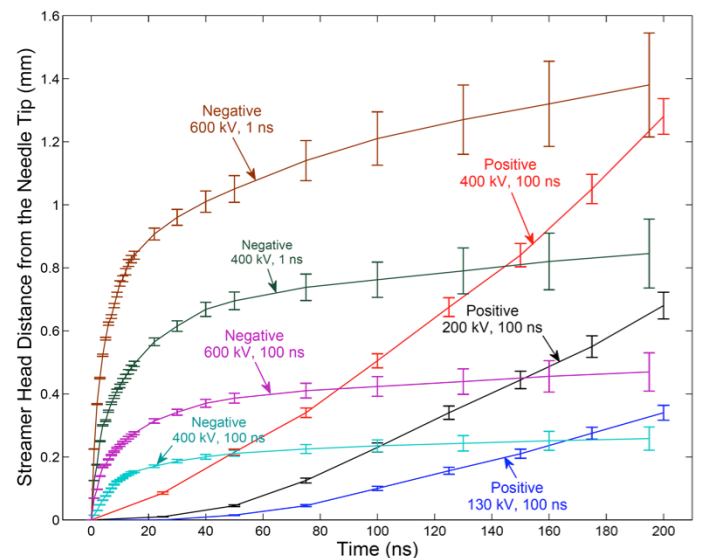


Figure 9: Streamer head average distance from needle tip for positive and negative applied voltages with different peak amplitudes. Positive streamer velocity tends to time increases, while a negative streamer decreases significantly after an initial bubble is formed around the needle. Error-bars show the range of results obtained by each of the artificial streamline diffusions (anisotropic, compensated streamline upwind Petrov-Galerkin and Galerkin least-square methods) to solve the charge continuity equations. The streamer velocity under +400 kV is roughly 2 times greater than +200 kV streamer velocity which is itself 2 times greater than +130 kV. Dissimilar rise-times for positive and negative streamers are shown to ease comparison between positive and negative streamers with velocities on the same order.

IV. EFFECTS OF RISE-TIME

Unfortunately, there is not enough experimental evidence to clarify the effects of the applied voltage rise and fall times on the shape and velocity of positive and negative streamers in dielectric liquids. Briels *et al.*, have shown in [22] and [23] that the applied voltages with shorter rise-times create streamers with visibly larger diameters in gaseous media. Our model shows that impulses with steeper rises form thicker positive and negative streamer columns in transformer oil as well (see definition of 10%-90% rise-time of applied impulse voltage defined by IEC in [9]). It is already shown that increasing the applied voltage magnitude rises both the initial ionized volume and the eventual streamer column diameter (Figs. 3-9). The effects of applied voltage rise-time on the positive streamer shape can be seen in Figs. 4, 10-13 for positive streamers and in Fig. 14 for negative streamers. The greater streamer diameter formed by steeper applied voltages is caused by the fact that shorter rise-times (higher rate of rise of electric field intensity) impose a stronger electrical ionization shock, especially around the needle. A faster rising electric field prevents the highly mobile electrons to diffuse into the bulk oil and by capturing more electrons over a larger volume forms a bulkier initial ionized volume, which ends up with a greater streamer column diameter. We have observed such phenomena in different polarities and peak amplitudes. For conciseness, the effects of the rise-time are shown only on the positive streamers formed by applied voltages with +200 kV peak amplitudes in Figs. 4, 10-13 and for the negative streamers formed by applied voltages with -400 kV and -600 kV peak amplitudes in Fig. 14. The positive streamer shown in Fig. 10 is slightly thicker compared to the one that is formed with longer rise-time as shown in Fig. 4. The difference between streamer diameters is more evident for the positive streamers formed by +200 kV impulse voltages with 10 ns and 1 ns rise-times shown in Figs. 11 and 12, respectively. Comparing Figs. 4, 10, 11 and 12 also suggests that the maximum electric field at the streamer head is slightly less ahead of the streamers formed by steeper applied voltages. Such drops in electric field magnitude are mainly caused by greater radii of curvature of the streamer heads formed by shorter rise-times. The other fact that contributes to the drops in electric field in thicker streamers is that the maximum volume charge density is also less for streamers formed by positive applied voltages with smaller rise-times. Such drops in maximum electric field ahead of the streamer directly lessens the instantaneous streamer velocity, which can lead to lower the chance of total breakdown over the gap if the pulse width (fall time) is not sufficiently long. Our model predicts relatively similar positive streamer behavior for other positive applied voltage magnitudes, such as +130 kV and +400 kV.

Decreasing the applied voltage rise-time, also broadens the distribution of the highly ionized volume close to the needle which can be considered as increasing the chance of branching. For instance a streamer formed by an impulse applied voltage with +200 kV peak and 1 ns rise-time occupies much more radial space than the positive streamer shown in Fig. 4. The model must be extended to a full three-

dimensional geometry to involve the physics of streamer branching and at this point, based on 2-D axisymmetric models we can only evaluate the branching possibility which seems to be more for applied voltages with greater peak amplitudes and/or shorter rise-times.

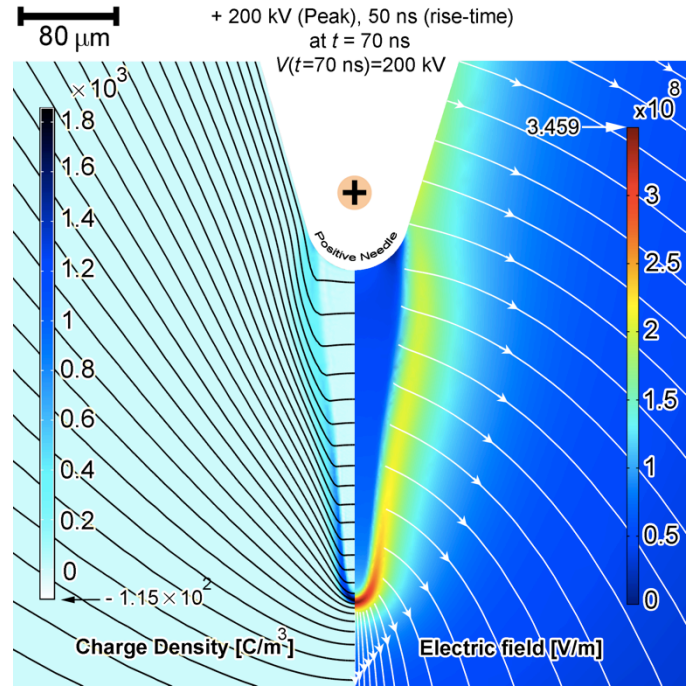


Figure 10: Electric field magnitude and lines (right side) and the net charge density and equipotential lines (left side) for a positively applied lightning impulse voltage with +200 kV peak and 50 ns rise-time at $t=70$ ns.

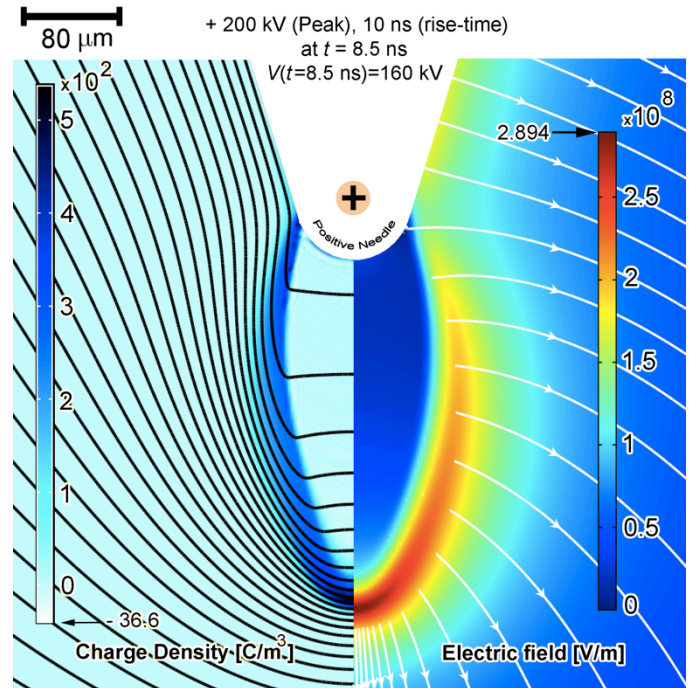


Figure 11: Electric field magnitude and lines (right side) and the net charge density and equipotential lines (left side) for a positively applied lightning impulse voltage with +200 kV peak and 10 ns rise-time at $t=8.5$ ns.

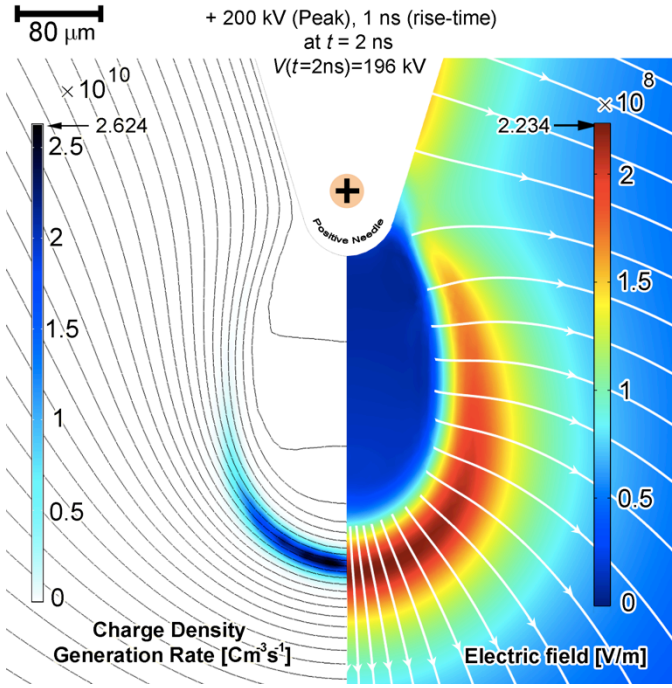


Figure 12: Electric field magnitude and lines (right side) and the net charge density and equipotential lines (left side) for a positively applied lightning impulse voltage with +200 kV peak and 2 ns rise-time at $t=2$ ns.

The diameter of the positive streamers gradually decreases when it elongates. The diameter reduction rate clearly depends on the applied voltage peak amplitude and rise-time. Figure 13 compares the positive streamer head radii of curvatures when the streamers travel a half-millimeter from the positive needle tip. It must be realized that the streamer head velocities, time instants, the instantaneous voltages are different for the cases shown in Fig. 13, however, the positions of the streamer heads are identical.

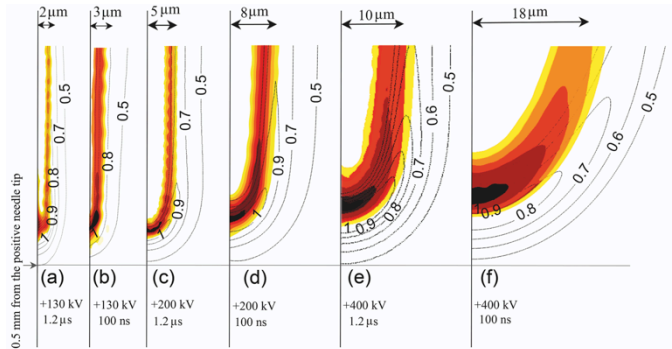


Figure 13: Volume charge densities and electric field distributions for different positively applied voltage peak amplitudes and rise-times. The pictures are shown for the instant times that the streamer heads travel half a millimeter from the needle tip. Space charge densities are shown as filled contours from $0.5|\rho_{max}|$ (the brightest color) to $|\rho_{max}|$ (the darkest color). Electric field contours are shown as black solid lines from $0.5|E_{max}|$ to $|E_{max}|$. The value of each contour is labeled on the curve as a fraction of $|E_{max}|$. The streamer head curvatures can be compared between streamers formed by (a): 130 kV with 1.2 μ s rise-time: $|E_{max}|=3.1 \times 10^8$ V/m, $|\rho_{max}|=4.25 \times 10^3$ C/m³; (b): 130 kV with 100 ns rise-time: $|E_{max}|=2.9 \times 10^8$ V/m, $|\rho_{max}|=3.94 \times 10^3$ C/m³; (c): 200 kV with 1.2 μ s rise-time: $|E_{max}|=2.9 \times 10^8$ V/m, $|\rho_{max}|=3.12 \times 10^3$ C/m³; (d): 200 kV with 100 ns rise-time: $|E_{max}|=2.8 \times 10^8$ V/m, $|\rho_{max}|=2.43 \times 10^3$ C/m³; (e): 400 kV with 1.2 μ s rise-time: $|E_{max}|=2.6 \times 10^8$ V/m, $|\rho_{max}|=1.54 \times 10^3$ C/m³; and (f): 400 kV with 100 ns rise-time $|E_{max}|=2.4 \times 10^8$ V/m, $|\rho_{max}|=0.93 \times 10^3$ C/m³.

Similar comparisons are also performed for the negative streamers in Fig. 14. Like positive streamers, increasing the applied voltage rise-time decreases the streamer volume over the same course of time. Comparing the right and left sides of Fig. 14 also shows that increasing the negatively applied voltage rise-time also decreases the radial velocity of the ionized bubble, which decreases the chance of branching. It also can be seen that increasing the applied voltage peak amplitude has a similar effect on the negative streamer volume as decreasing the applied voltage rise-time.

Increasing rise-time of the negatively applied voltages also decreases the maximum ionization rate, G_{max} and its gradient. It is visible for streamers formed by -400 kV peak and 100 ns rise-time. Regarding the streamers formed by -600 kV and 100 ns rise-time, it must be noted that the ionization rate is slightly less than $0.5|G_{max}|$ for points closer than 0.1 to the needle which are not shown in Fig. 14 to prevent confusion with a -400 kV, 100 ns negative streamer.

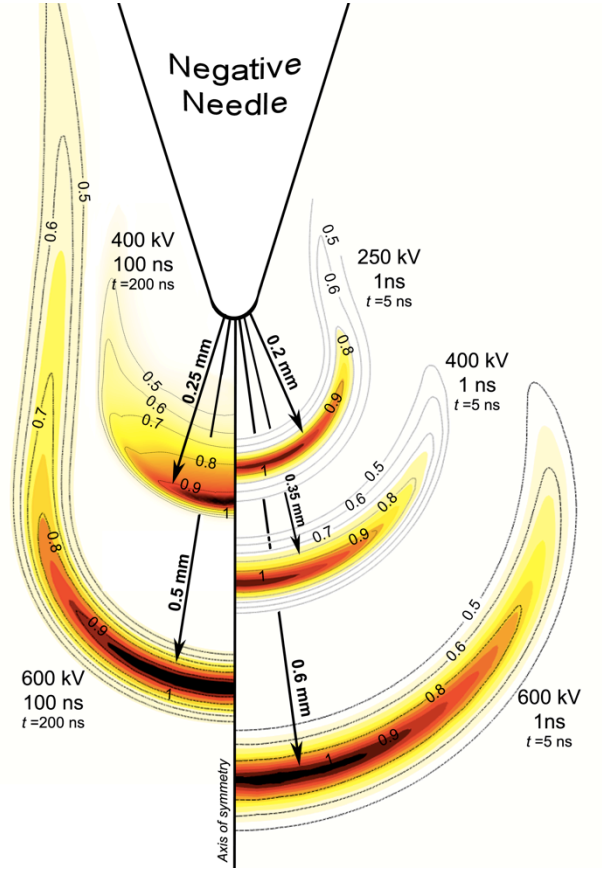


Figure 14: Electric field distributions and charge density generation rates for different negatively applied voltage peak amplitudes and rise-times. Space charge density generation rate, G_M are shown as filled contours from $0.5|G_{max}|$ (the brightest color) to $|G_{max}|$ (the darkest color). Electric field contours are shown as black solid lines from $0.5|E_{max}|$ to $|E_{max}|$. The value of each contour is labeled on the curve as a fraction of $|E_{max}|$. The approximate radius of an ionized bubble can be compared between different applied voltage peaks and rise-times: -250 kV with 1 ns rise-time (upper right): $|E_{max}|=1.01 \times 10^8$ V/m and $|G_{max}|=0.7 \times 10^{11}$ Cm⁻³s⁻¹; -400 kV with 1 ns rise-time (middle right): $|E_{max}|=1.42 \times 10^8$ V/m and $|G_{max}|=1.2 \times 10^{11}$ Cm⁻³s⁻¹; -600 kV with 1 ns rise-time (bottom right): $|E_{max}|=1.75 \times 10^8$ V/m and $|G_{max}|=6.21 \times 10^{11}$ Cm⁻³s⁻¹; -400 kV peak with 100 ns rise-time (upper left): $|E_{max}|=0.95 \times 10^8$ V/m and $|G_{max}|=0.84 \times 10^{11}$ Cm⁻³s⁻¹; and -600 kV peak with 100 ns rise-time (bottom left): $|E_{max}|=1.15 \times 10^8$ V/m and $|G_{max}|=1.21 \times 10^{11}$ Cm⁻³s⁻¹.

V. EFFECTS OF TRANSFORMER OIL PROPERTIES

Transformer oil is not a pure liquid hydrocarbon, but is a mixture of many different naphthenic, paraffinic, and aromatic molecules with a complex molecular structure. This feature of transformer oil makes it difficult to characterize many parameters, such as electron mobility. The electric field dependent molecular ionization is the key mechanism for streamer development in transformer oil. Except for the ionization potential function, we have imported the rest of the parameters into the model using simple assumptions with no or weak experimental records. Firstly, there are multiple evidence indicating that effective electron mass, m^* is a function of electric field while we have imported a constant value for zero electric field due to the lack of reference. It is fairly complicated to derive a function for effective mass of free electrons [24], which is in the scope of this research. Secondly, the number of the ionizable species, n_0 , is not really known for different situations of transformer oil. The previous works have assumed empirical values for n_0 [5], [6]. The model results indicate that there is a semi-linear relation between numbers of ionizable species, n_0 , and the streamer velocity. The number of ionizable species, n_0 , has been simply increased to model higher modes of positive streamers in [25], however, as discussed in Section III, the 3rd mode positive streamer velocity only rises an order of magnitude when the streamer reaches 8~10 mm from the needle tip [2]. Therefore, it seems that n_0 is a function of electric field intensity itself, which is not known to the best of the authors' knowledge.

The third important parameter, which is not known precisely, is the electron mobility. The value, shown in Table I for electron mobility is derived from Walden's rule, which assumes the electron is a spherical particle and uses a classical electron radius, R_e known as the Lorentz radius [5]. However, a simple dependence of particle mobilities on the bulk oil temperature [1] applied to the model has significantly increased the negative streamer velocity [14].

The temperatures obtained in the model for streamer core, indicate that a gas (vapor) phase develops underneath the streamer crust due to collisions. The model does not cover the ionization process in the gas phase. Future studies should include impact ionization in gas phase as well as liquid bulk [26, 27] to better model the pre-breakdown mechanisms behind streamer propagation.

As a conclusion, the exact parameters describing the actual behavior of the hydrocarbon molecules in the pre-breakdown stage are not fully known and there is still much work remaining to be done on the characteristics of the transfer oil molecule under electrical and thermal stresses.

VI. CONCLUSION

Mechanisms behind the positive and negative streamers formed by standard impulse voltages with different peak amplitudes and rise-times have been compared using an electro-thermal hydrodynamic model. Simulation results indicate that negative streamers demand higher peak voltages to initiate from a needle electrode. Also, bushy negative streamers initially occupy larger volume around the needle electrode compared to the filamentary positive streamers. An

initial ionized body formed by negatively applied impulse voltage propagates slower due to the lower electric field enhancement ahead of the ionized region. When the ionized body grows a few millimeters from the negative needle, the 2-D axisymmetric model fails to track the physical velocity of the negative streamer, since in spite of positive streamers, experiments confirm that the negative streamers cannot propagate in a stable single on-axis streamer column and the formation of the off-axis branches are inevitable for negative streamer propagation beyond a few millimeters. Branching phenomena must be studied in a computationally expensive full 3-D model, which is in the scope of this continuing research. Including the electric field dependence of ionization potential derived using DFT [7], [11] enables the presented model to physically describe the higher streamer velocity and streamer column diameter under higher applied voltages. The model confirms that higher mode velocities do not take place until the streamer travels beyond 8~10 millimeters from the needle electrode as already observed in experiments [2].

Our model also indicates that the applied voltages with smaller rise-times form thicker streamer columns in liquid dielectrics, while applied voltages with longer rise-times create thinner streamers. Such effects have been reported from experiments on the streamer formed in gaseous media.

The molecular structure and behavior of liquids is more complex than gases and solids and even in the purest liquids there exists trace amounts of impurities that make it difficult to isolate the mechanisms behind electrical breakdown. In particular, transformer oil is a mixture of many different aromatic, naphthenic, and paraffinic molecules with complex molecular structures. The major weak point of the presented model is the lack of data about effective electron mass, electron mobility and number of ionizable species in electrically stressed transformer oil.

ACKNOWLEDGMENT

This work has been supported by ABB Corporate Research, Västerås, Sweden.

REFERENCES

- [1] V. Y. Ushakov, V. F. Klimkin, and S. M. Korobeynikov, *Impulse Breakdown of Liquids*. Springer-Verlag, Berlin, 2007.
- [2] L. Lundgaard, D. Linhjell, G. Berg, and S. Sigmond, "Propagation of positive and negative streamers in oil with and without pressboard interfaces," *IEEE Trans. Dielectr. Electr. Insul.*, vol. 5, pp. 388-395, 1998.
- [3] O. Lesaint and G. Massala, "Positive streamer propagation in large oil gaps: experimental characterization of propagation modes," *IEEE Trans. Dielectr. Electr. Insul.*, vol 5, pp. 360-370, June 1998.
- [4] V. Segal, A. Hjortsberg, A. Rabinovich, D. Nattrass, K. Raj, "AC (60Hz) and impulse breakdown strength of a colloidal fluid based on transformer oil and magnetite nanoparticles," *IEEE International Symposium on Electrical Insulation*, pp.619-622, Arlington, VA, 1998.
- [5] F. O'Sullivan, A model for the initiation and propagation of electrical streamers in transformer oil and transformer oil based nanofluids, *Ph.D. dissertation, Massachusetts Institute of Technology (MIT)*, Cambridge, MA, USA, 2007.
- [6] J. G. Hwang, Elucidating the mechanisms behind pre-breakdown phenomena in transformer oil systems, *Ph.D. dissertation, Massachusetts Institute of Technology (MIT)*, Cambridge, MA, USA, 2010.

- [7] H. S. Smalø, Ø. Hestad, S. Ingebrigtsen, and P. O. Åstrand, "Field dependence on the molecular ionization potential and excitation energies compared to conductivity models for insulation materials at high electric fields," *J. Applied Phys.*, 109, 109, 073306, 2011.
- [8] IEC Standard #60897, "Methods for the determination of the lightning impulse breakdown voltage of insulating liquids."
- [9] IEC Standard # 60060-1, "High-voltage test techniques - Part 1: General definitions and test requirements."
- [10] J. Qian, R. P. Joshi, E. Schamiloglu, J. Gaudet, J. R. Woodworth, and J. Lehr, "Analysis of polarity effects in the electrical breakdown of liquids," *J. Phys. D: Appl. Phys.*, Vol. 39, pp. 359-369, 2006.
- [11] C. Zener. A theory of the electrical breakdown of solid dielectrics. Proc. Roy. Soc. A, pp. 523-529, 1934.
- [12] David S. Sholl, Jangie A. Steckel, *Density Functional Theory, A Practical Introduction*, John Wiley & Sons, Inc., New Jersey, 2009.
- [13] R. Codina, "A discontinuity-capturing cross-wind-dissipation for the finite element solution of the convection-diffusion equation," *Computer Methods in Applied Mechanics and Eng.*, vol. 110, pp. 325-342, 1993.
- [14] Reference guide COMSOL Multiphysics 4.2.
- [15] J. Jadidian, J. G. Hwang, M. Zahn, N. Lavesson, O. Widlund, K. Borg, "Streamer Initiation and Propagation in Transformer Oil under Positive and Negative Impulse Voltages," *13th IEEE Int. Pulsed Power Conf.*, Chicago, USA, June 2011.
- [16] J. Jadidian, J. G. Hwang, M. Zahn, N. Lavesson, O. Widlund, K. Borg, "Streamer Dynamics in Transformer Oil: Influence of Applied Voltage Rise Time," *38th IEEE Int. Conf. on Plasma Science*, Chicago, USA, June 2011.
- [17] J. C. Devins, S. J. Rzd, R. J. Schwabe, "Breakdown and prebreakdown phenomena in liquids," *J. Appl. Phys.* 52(7), 1981.
- [18] K. C. Kao, J. P. C. McMath, "Time dependent pressure effect in liquid dielectrics," *IEEE Trans. Elec. Insul.*, vol. EI-5, no. 3, pp. 64-68, 1970.
- [19] M. Cevallos, M. Butcher, J. Dickens, A. Neuber, H. Krompholz, "Imaging of Negative Polarity DC Breakdown Streamer Expansion in Transformer Oil due to Variations in Background Pressure," *IEEE Trans on Plasma Sci.*, vol. 33, pp 494-495, 2005.
- [20] O. Lesaint, R. Tobazeon, "Streamer Generation and Propagation in Transformer Oil under ac Divergent Field Conditions," *IEEE Trans. Electr. Ins.*, vol. 23, no. 6 pp. 941-954, 1988.
- [21] E. M. van Veldhuizen, P. C. M. Kemps, and W. R. Rutgers, "Streamer Branching in a Short Gap: The Influence of the Power Supply," *IEEE Trans on Plasma Sci.*, vol. 30, no. 1, pp 162-163, 2002.
- [22] T. M. P. Briels, E. M. van Veldhuizen, U. Ebert, "Positive streamers in air and nitrogen of varying density: experiments on similarity laws," *J. Phys. D, Applied Phys.*, vol. 41, 234008 (14pp), 2008.
- [23] T. M. P. Briels, *et al.*, "Positive and negative streamers in ambient air: measuring diameter, velocity and dissipated energy," *J. Phys. D, Applied Phys.*, vol. 41, 234004 (11pp), 2008.
- [24] G. Giuliani, G. Vignale, *Quantum Theory of the Electron Liquid*, Cambridge University Press, Cambridge-UK, 2005.
- [25] J. G. Hwang, M. Zahn, L. A. A. Pettersson, O. Hjortstam, R. Liu, "Modeling Streamers in Transformer Oil: The Transitional Fast 3rd Mode Streamer," *IEEE 9th International Conference on Properties and Applications of Dielectric Materials*, pp. 573-578, 2009.
- [26] J. Jadidian, S. Mohseni, M. Jebeli-Javan, E. Hashemi, A. A. Shayegani, K. Niayesh, "Visualization of a Copper Wire Explosion in Atmospheric Pressure Air," *IEEE Transactions on Plasma Science*, Vol. 39, No. 11, pp. 2842 – 2843, Nov. 2011.
- [27] J. Jadidian, "A Compact Design for High Voltage Direct Current Circuit Breaker," *IEEE Transactions on Plasma Science*, Vol. 37, No. 6, pp. 1084 – 1091, Jun. 2009.



Jouya Jadidian (S'06) received the B.Sc. and M.Sc. degrees in electrical engineering from the University of Tehran, Tehran, Iran, in 2006 and 2008, respectively. He is currently working towards the Ph.D. degree in the Department of Electrical Engineering and Computer Science at the Massachusetts Institute of Technology (MIT), Cambridge, MA.

Since 2004 to 2010, he has been with the High Voltage and Pulsed Power Research Institute, University of Tehran. Since 2007, he has also been

with the Iranian Grid Management Company, Tehran, in the "High Voltage Transmission System and Power System Protection" office as a Consultant. His current research interests include electrical breakdown in vacuum, gases

and liquids. He has contributed to over 40 technical publications in journals and international conference proceedings.

Mr. Jadidian was the recipient of the 2010 IEEE NUCLEAR AND PLASMA SCIENCE SOCIETY Graduate Scholarship Award and 2011-12 IEEE DIELECTRICS AND ELECTRICAL INSULATION SOCIETY Fellowship Award.



Markus Zahn (S'68–M'71–SM'78–F'93) received the B.S.E.E., M.S.E.E., electrical engineer, and D.Sc. degrees in electrical engineering from the Massachusetts Institute of Technology (MIT), Cambridge, MA, in 1968, 1968, 1969, and 1970, respectively.

He then joined the Department of Electrical Engineering, University of Florida, Gainesville, until 1980 when he returned to MIT, where he is now Professor of Electrical Engineering working in the

Research Laboratory of Electronics, Laboratory for Electromagnetic and Electronic Systems and the High Voltage Research Laboratory. He is also the Director of the MIT Course VI-A EECS Internship Program, a cooperative work/study program with industry. He is the author of *Electromagnetic Field Theory: A Problem Solving Approach* (now out of print) but is working on a new reference book with a complete collection of solved electromagnetism problems. He has received numerous excellences in teaching awards at the University of Florida and MIT. His primary research areas are ferrohydrodynamics and electrohydrodynamics for microfluidic, biomedical and micro/nano electromechanical system (MEMS/NEMS) applications, nanoparticle technology for improved high-voltage performance of electric power apparatus, Kerr electro-optic field and space charge mapping measurements in high-voltage stressed materials, and for the development of model-based interdigital dielectrometry and magnetometry sensors. He is a co-Inventor on 19 patents. He has contributed to about 10 book and encyclopedia chapters, about 115 journal publications, and about 175 conference papers.

Prof. Zahn was a Distinguished Visiting Fellow of the Royal Academy of Engineering at the University of Manchester, Manchester, U.K.; the 1998 J.B. Whitehead Memorial Lecturer; the first James R. Melcher Memorial Lecturer in 2003 and was the 2011 Inuishi Memorial Lecturer of the 2011 International Symposium on Electrical Insulating Materials (ISEIM). He is an Associate Editor of the IEEE TRANSACTIONS ON DIELECTRICS AND ELECTRICAL INSULATION, is on the International Scientific Committee on Magnetic Fluids, and has received a Certificate of Achievement for completion of the "Deminers Orientation Course" at the Night Vision and Electronic Sensors Directorate Countermeasures Division, Ft. Belvoir, VA.



Nils Lavesson received a M.Sc. degree in engineering physics and a Ph.D. in theoretical physics from Lund University, Lund, Sweden, in 2004 and 2009 respectively. He then joined the Department of High Voltage Engineering at Chalmers University of Technology in Gothenburg, Sweden, as a postdoctoral researcher. He joined ABB Corporate Research in Västerås, Sweden, in 2010.



Ola Widlund received a M.Sc. in engineering physics in Lund, Sweden, in 1990. After a few years in industry he returned to academia, resulting in a Ph.D. in fluid mechanics at the Royal Institute of Technology, Stockholm, in 2000. He did a two-year post-doc at CNRS in Grenoble (France) with a Marie Curie Fellowship, followed by two years at CEA in Grenoble as a guest researcher. He moved back to Sweden and joined ABB Corporate Research in 2005.



Karl Borg received a M.Sc. in physics in Stockholm, Sweden, in 1998, and a Ph.D. in kinetic theory of gases at the Royal Institute of Technology, Stockholm, in 2003. He did a post-doc at Kyoto University (Japan) in 2006 and another post-doc at University of Limerick (Ireland) in 2009. He joined ABB Corporate Research in 2010.